Electronic Supplementary Material:

Genetic variation underlies plastic responses to global change drivers in the purple sea urchin, *Strongylocentrotus purpuratus*.

Marie E. Strader[1,2†], Matthew E. Wolak[1†], Olivia M. Simon[2], Gretchen E. Hofmann[2]

[1]Department of Biological Sciences, Auburn University

[2]Department of Ecology, Evolution and Marine Biology, University of California Santa Barbara

[†]Contributed equally to this study.

Manuscript published as a Research Article in *Proceedings of the Royal Society B: Biological Sciences*

Contents

All data and R code for this study are available in a version controlled repository on GitHub at https://github.com/qgevoeco/QGplasticity_S_purpuratus

1. Rearing conditions and experimental design

Table S1. Adult urchins were collected by hand on SCUBA at Naples (34.4221216, -119.95154) on August 23, 2018, and from Arroyo Quemado (34.46774988, -120.11905) on September 21, 2018. Average salinity and TA for the duration on the adult acclimation and culturing period was 33.2 ± 0.1 ppt and 2233 ± 4 μmol k^{-1}, respectively.

		pH_{total}	pCO_2 (μatm)	Ω_{Arg}	Temperature (˚C)
Adult Treatment	Upwelling (U)	7.64 ± 0.07	1117 ± 191	0.93 ± 0.14	12.8 ± 0.28
	Nonupwelling (N)	7.89 ± 0.07	596 ± 102	1.84 ± 0.24	17.0 ± 0.12
Developmental Treatment	Upwelling (U)	7.73 ± 0.06	886 ± 120	1.15 ± 0.12	13.2 ± 0.47
	Nonupwelling (N)	8.01 ± 0.01	437 ± 8	2.28 ± 0.04	17.0± 0.24

Supplemental Methods:

Site details: Adult urchins were collected by hand on SCUBA at Naples reef, a shale outcrop within the Santa Barbara Channel (34.4221216, -119.95154) on August 23, 2018. Urchins (N=118) were transported to a seawater facility at UCSB and held in flow-through ambient seawater prior to adult conditioning beginning on September 4, 2018. After slight mortality directly after collection, urchins were consolidated into 3 tanks per treatment and a second set of urchins (N=10) was collected at Arroyo Quemada (AQ), another long-term site monitored through the SBC (34.46774988, -120.11905) on September 21, 2018. These sites share similar habitat quality and *S. purpuratus* abundances [1]. Ten AQ urchins were immediately added to two separate tanks, one per treatment (10 AQ urchins per treatment, tank IDs N4, and U4).

Water Chemistry: Temperature and pCO_2 levels were maintained throughout the conditioning period using heat pumps regulated by Nema 4X digital temperature controllers and a flow-through CO_2 mixing system, modified from Fangue et al. [2]. Treated seawater was evenly pumped from two reservoir tanks to conditioning tanks at a rate of 20L/hr. Temperature and pH values were taken every day using an Omega HH81A thermocouple and durafet sensors [3]. Spectrophotometric pH and salinity measurements were taken twice a week following best practices outlined in Dickson [4]. Samples for total alkalinity were taken once a week and measured using titration following established protocols [4]. Carbonate chemistry parameter values were calculated using CO_2calc [5] and either durafet measured pH or spectrophotometric pH with associated salinity, temperature and total alkalinity values and equilibrium constants [6,7]. For larval cultures, temperatures and durafet pH measurements of reservoir tanks were taken every day while spectrophotometric pH and salinity measurements were taken from each individual culture when larvae were 24-hour post fertilization (hpf).

Urchin spawning: Urchins were induced to spawn using intracoelemic injections of 0.53M KCl. Eggs were collected with UV sterilized 0.35um filtered seawater (FSW) while sperm was collected dry and stored on ice until activation with FSW. Test fertilizations were performed to verify gamete compatibility and ensure at least 95% fertilization success between chosen males

and females. All spawned urchins (N=40) originated from Naples Reef, except for the following: N1, N2, N4, N9, N10, U9, U10 (females), and N9, N10, U9, U10 (males), which originated from Arroyo Quemado.

References:

1. Castorani, M. C. N., Harrer, S. L., Miller, R. J. & Reed, D. C. Disturbance structures canopy and understory productivity along an environmental gradient. *Ecol. Lett.* **24**, 2192–2206 (2021).
2. Fangue, N. A., O'Donnell, M. J., Sewell, M. A., Matson, P. G., MacPherson, A. C. & Hofmann, G. E. 2010 A laboratory-based, experimental system for the study of ocean acidification effects on marine invertebrate larvae. *Limnol. Oceanogr. Methods* **8**, 441–452. (doi:10.4319/lom.2010.8.441)
3. Kapsenberg, L., Bockmon, E. E., Bresnahan, P. J., Kroeker, K. J., Gattuso, J.-P. & Martz, T. R. 2017 Advancing Ocean Acidification Biology Using Durafet® pH Electrodes. *Front. Mar. Sci.* **4**, 1–9. (doi:10.3389/fmars.2017.00321)
4. Dickson, A. G., Sabine, C. L. & Christian, J. R. 2007 *Guide to Best Practices for Ocean CO 2 Measurements*.
5. Robbins, L. L., Hansen, M. E., Kleypas, J. A. & Meylan, S. C. 2010 CO2calc: A User-Friendly Seawater Carbon Calculator for Windows, Mac OS X, and iOS (iPhone). *Open-File Rep.*
6. Mehrbach, C., Culberson, C. H., Hawley, J. E. & Pytkowicx, R. M. 1973 Measurement of the Apparent Dissociation Constants of Carbonic Acid in Seawater At Atmospheric Pressure. *Limnol. Oceanogr.* **18**, 897–907. (doi:10.4319/lo.1973.18.6.0897)
7. Dickson, A. G. & Millero, F. J. 1987 A comparison of the equilibrium constants for the dissociation of carbonic acid in seawater media. *Deep Sea Res.* **34**, 1733–1743. (doi:10.1002/1099-0518(20010315)39:6<872::AID-POLA1061>3.0.CO;2-I)

2. Model outputs

Table S2. *Strongylocentrotus purpuratus* spicule length marginal posterior mode, mean (in square brackets), and 95% credible interval limits (in parentheses) as estimated for Non-Upwelling (N) or Upwelling (U) developmental environments in either the model for Non-Upwelling parental environment (top two rows) or Upwelling parental environment (bottom two shaded rows). Within the additive genetic matrices, development-specific additive genetic variances (V_A) are shown along the diagonal with cross-developmental environment covariances (COV_A) and correlations (r_A) above and below the diagonal, respectively. Sire, Dam, Culture, and Block variances were jointly estimated for both development environments and are only indicated in the first row for each model.

Environment		**Additive Genetic Matrix**		**Sire**	**Dam**	**Culture**	**Block**	**Residual**	**heritability**	**evolvability**
Parent	Development	Development N	Development U							
N	N	V_A=0.00425 [0.295] (1.51×10^{-10},0.958)	COV_A=-0.000268 [0.104] (-0.344,0.686)	0.177 [0.245] (7.27×10^{-8},0.712)	0.00272 [0.0994] (7.44×10^{-8},0.350)	0.0802 [0.0839] (0.0403,0.137)	0.0483 [0.349] (1.67×10^{-7},1.26	0.975 [0.858] (0.506,1.08)	0.00305 [0.157] (6.32×10^{-11}, 0.475)	4.21×10^{-5} [0.00205] (1.15×10^{-12},0.00669)
N	U	r_A=0.232 [0.118] (-0.663,0.814)	V_A=1.20 [1.42] (0.339,2.69)					0.974 [1.00] (0.389,1.57)	0.425 [0.454] (0.125,0.794)	0.0145 [0.0182] (0.00448,0.0355)
U	N	V_A=0.00694 [0.351] (4.59×10^{-7},1.05)	COV_A=-0.00559 [0.0725] (-0.288,0.564)	0.00161 [0.108] (8.81×10^{-11},0.390)	0.126 [0.281] (4.76×10^{-7},0.783)	0.0680 [0.0774] (0.0370,0.126)	0.223 [0.823] (2.25×10^{-7},2.97)	0.991 [0.864] (0.499,1.1)	0.00337 [0.163] (2.84×10^{-7},0.474)	4.42×10^{-5} [0.00230] (2.90×10^{-9},0.00680)
U	U	r_A=0.268 [0.0714] (-0.749,0.746)	V_A=0.676 [0.758] (2.01×10^{-6},1.61)					1.01 [0.893] (0.441,1.29)	0.267 [0.295] (8.42×10^{-7},0.602)	0.00785 [0.00692] (1.89×10^{-8},0.0148)

Table S3. *Strongylocentrotus purpuratus* body length marginal posterior mode, mean (in square brackets), and 95% credible interval limits (in parentheses) as estimated for Non-Upwelling (N) or Upwelling (U) developmental environments in either the model for Non-Upwelling parental environment (top two rows) or Upwelling parental environment (bottom two shaded rows). Within the additive genetic matrices, development-specific additive genetic variances (V_A) are shown along the diagonal with cross-developmental environment covariances (COV_A) and correlations (r_A) above and below the diagonal, respectively. Sire, Dam, Culture, and Block variances were jointly estimated for both development environments and are only indicated in the first row for each model.

Environment		**Additive Genetic Matrix**		**Sire**	**Dam**	**Culture**	**Block**	**Residual**	**heritability**	**evolvability**
Parent	Development	Development N	Development U							
N	N	V_A=0.101 [0.252] (2.17×10^{-7},0.656)	COV_A=-0.000310 [-0.0106] (-0.148,0.125)	0.000199 [0.0191] (3.03×10^{-9},0.0760)	0.0772 [0.174] (1.05×10^{-5},0.455)	0.0508 [0.0537] (0.0275,0.0853)	0.0314 [0.205] (2.23×10^{-8},0.828)	0.687 [0.625] (0.390,0.775)	0.129 [0.191] (1.36×10^{-7},0.464)	5.71×10^{-4} [0.00113] (9.45×10^{-10},0.00291)
N	U	r_A=-0.228 [-0.151] (-0.871,0.630)	V_A=0.00326 [0.147] (8.48×10^{-8},0.466)					0.561 [0.521] (0.353,0.630)	0.00190, [0.141] (9.52×10^{-8},0.423)	1.17×10^{-5} [0.000854] (4.76×10^{-10},0.00267)
U	N	V_A=0.00250 [0.0991] (5.31×10^{-7},0.358)	COV_A=0.000429 [0.0231] (-0.0495,0.136)	0.00186 [0.0729] (9.68×10^{-10},0.235)	0.0242 [0.106] (3.93×10^{-7},0.316)	0.128 [0.135] (0.0820,0.195)	0.0374 [0.291] (3.22×10^{-7}, 1.00]	0.804 [0.789] (0.635,0.902)	0.000738 [0.0705] (3.52×10^{-7},0.251)	1.00×10^{-5} [0.000431] (2.34×10^{-9},0.00155)
U	U	r_A=0.651 [0.187] (-0.614,0.966)	V_A=0.000501 [0.0659] (4.32×10^{-8},0.253)					0.641 [0.616] (0.504,0.696)	0.000857 [0.0553] (4.16×10^{-8},0.205)	2.86×10^{-6} [0.000357] (2.37×10^{-10},0.00138)

3. Parental effects on egg size and treatment effects on development

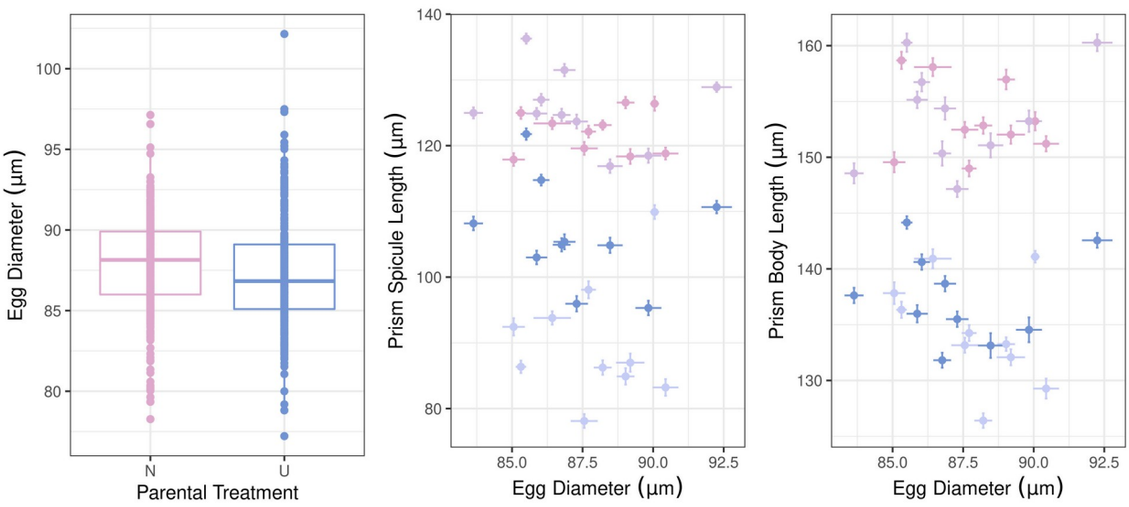

Figure S1. Egg diameter measured for each dam (N=35eggs/dam, 10 dams per treatment). Relationship between egg diameter and prism morphometrics for each dam (dot) (+/- 1 standard error).

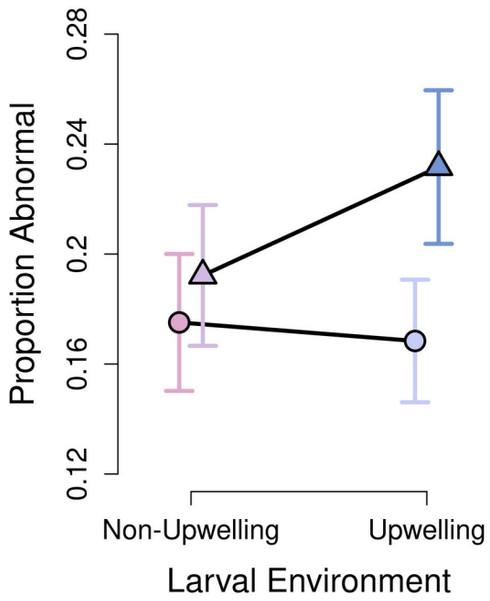

Figure S2. Mean proportion abnormality (error bars represent +/-1 standard error of the mean) of larvae randomly sampled in each culture prior to sampling at the prism stage. Larval morphometrics were scored only on fully developed prism larvae. Parents were either conditioned in the non-upwelling (circles) or upwelling (triangles) environments (black solid lines connect treatment means from the same parental environment). Colors refer to treatment combinations as detailed in figure 1.

4. Inference and Interpretation

Inference across full probability distributions

Our inferences consider the full probability distributions of the parameters, or in other words the posterior distributions give us the probabilities that a given parameter estimate takes on each value in our model after incorporating the data. With a frequentist confidence interval, the true parameter estimate can take on any value between confidence interval limits with no indication of which of the values between the limits is closer to that true parameter value. However, Bayesian credible intervals (and when considered alongside full posterior probability distributions) give information as to the probability of the parameter estimate along the possible parameter values contained by the credible interval limits. To aid in this interpretation, we also include figures that depict the full probability distributions of parameters that hold the most biological importance in this manuscript. Therefore, inference about parameters is done considering the entire probability distribution instead of just a few numbers used to summarize the entire uncertainty.

Extending this idea, we draw inference about the differences between parameters directly instead of comparing whether 95% credible intervals overlap. Using full probability distributions allow uncertainty in parameter estimates to be used when calculating other parameters of interest, such as a difference between model estimates of phenotypic mean in one treatment versus another (e.g., Figure 2 in the main text) or the difference between evolvability of one treatment versus another. Such calculations are done across the full probability distributions of both parameters (e.g., the difference is calculated for each Markov Chain Monte Carlo sample) and yields a full probability distribution for the difference (e.g., the difference calculated across each MCMC sample represents the full posterior probability distribution of the difference). This enables us to interpret the difference between model parameters in a way that is meaningful in the context of parameter estimation and is also biologically meaningful. For example, differences between model estimated mean spicule lengths of two treatments can be compared to a meaningful percentage of the trait's original size. Similarly, if the question is whether two parameters differ from one another (e.g., are two additive genetic variances different) we calculate the probability that the difference between these parameters is greater than zero. This is subtly different, but more informative, than a frequentist null hypothesis test that evaluates the null hypothesis that the difference equals zero.

Variance component credible interval limits

Interpretation of variance component credible intervals (CI) that converge toward zero is done considering that variances of random effects in linear mixed models are not allowed to be zero (in practice, variances are constrained to be above a small number that is set as the limit for an "effective zero"). Consequently, variance parameter estimates, and their uncertainty can never be evaluated at exactly zero. With Bayesian inference particularly, the marginal posterior distribution of a parameter indicates the modeled probability of each parameter value, after observing the data and controlling for uncertainty in all other model parameters. Because the uncertainty is truncated at an effective zero, we instead describe the shape of the posterior near zero. Variance parameter lower credible interval (CI) limits that converge to zero describe situations where both the lower CI limit and a large proportion of the marginal posterior probability density are located very near the effective zero. This is contrasted to a lower CI limit that does not converge to zero but may also be located near zero in a thin tail of the distribution (i.e., very little probability density in the area near the lower CI limit). In the latter case, the lower credible interval limit is not described as converging to zero.

5. Variance component prior and posterior distributions

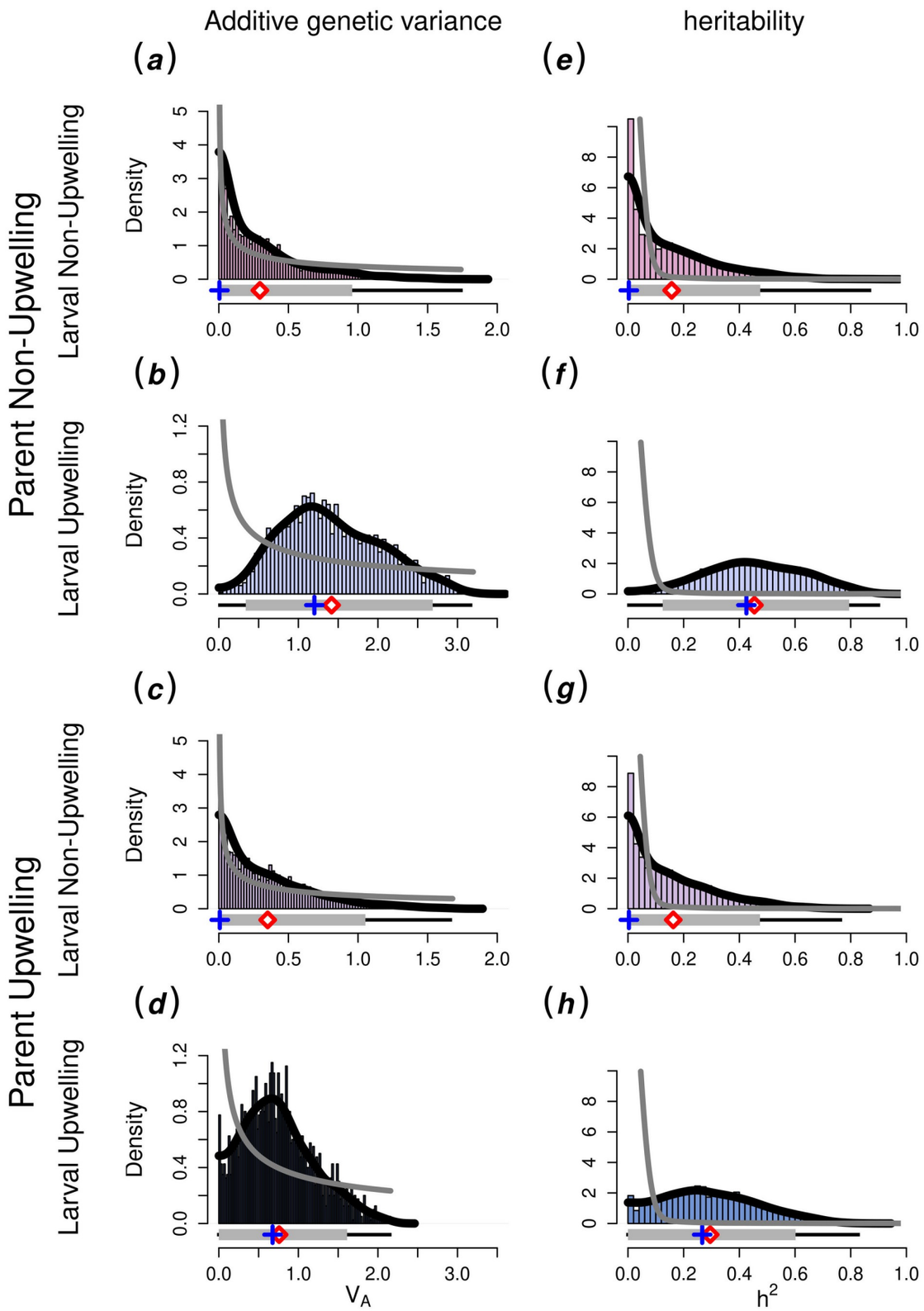

Figure S3: *S. purpuratus* spicule length marginal posterior MCMC samples (histogram bars with sample range depicted underneath by the thin black line), kernel density estimate (black line), posterior mean (red diamond) and mode (blue cross), 95% credible interval (grey bar), and prior density (grey line) for the additive genetic variance (V_A) (*a-d)* and heritability (h^2) (*e-h*). Colors refer to treatment combinations as detailed in figure 1.

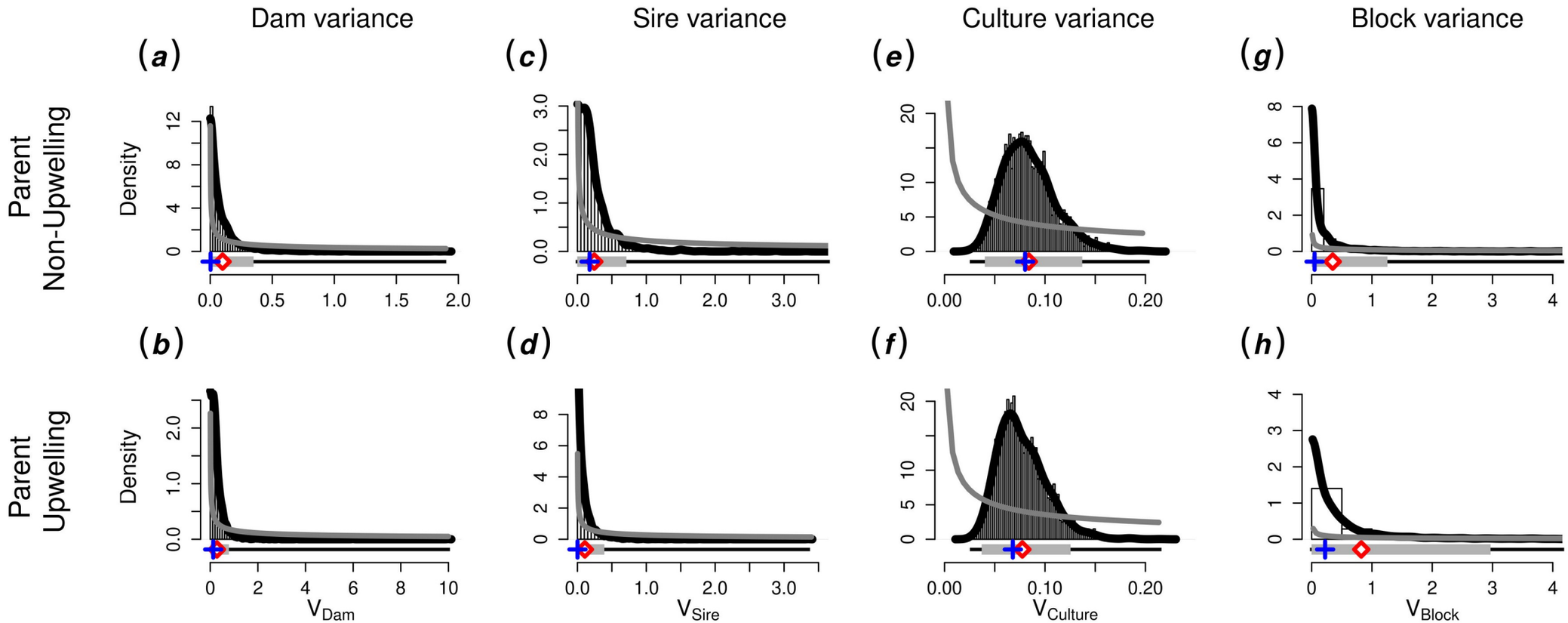

Figure S4. *S. purpuratus* spicule length marginal posterior MCMC samples, (histogram bars with the range of samples depicted underneath by the thin black line), kernel density estimate (black line), posterior mean (red diamond) and mode (blue cross), 95% credible interval (grey bar), and prior density (grey line) for the dam (*a*-*b*), sire (*c*-*d*), culture (*e*-*f*), and block (*g*-*h*) variances.

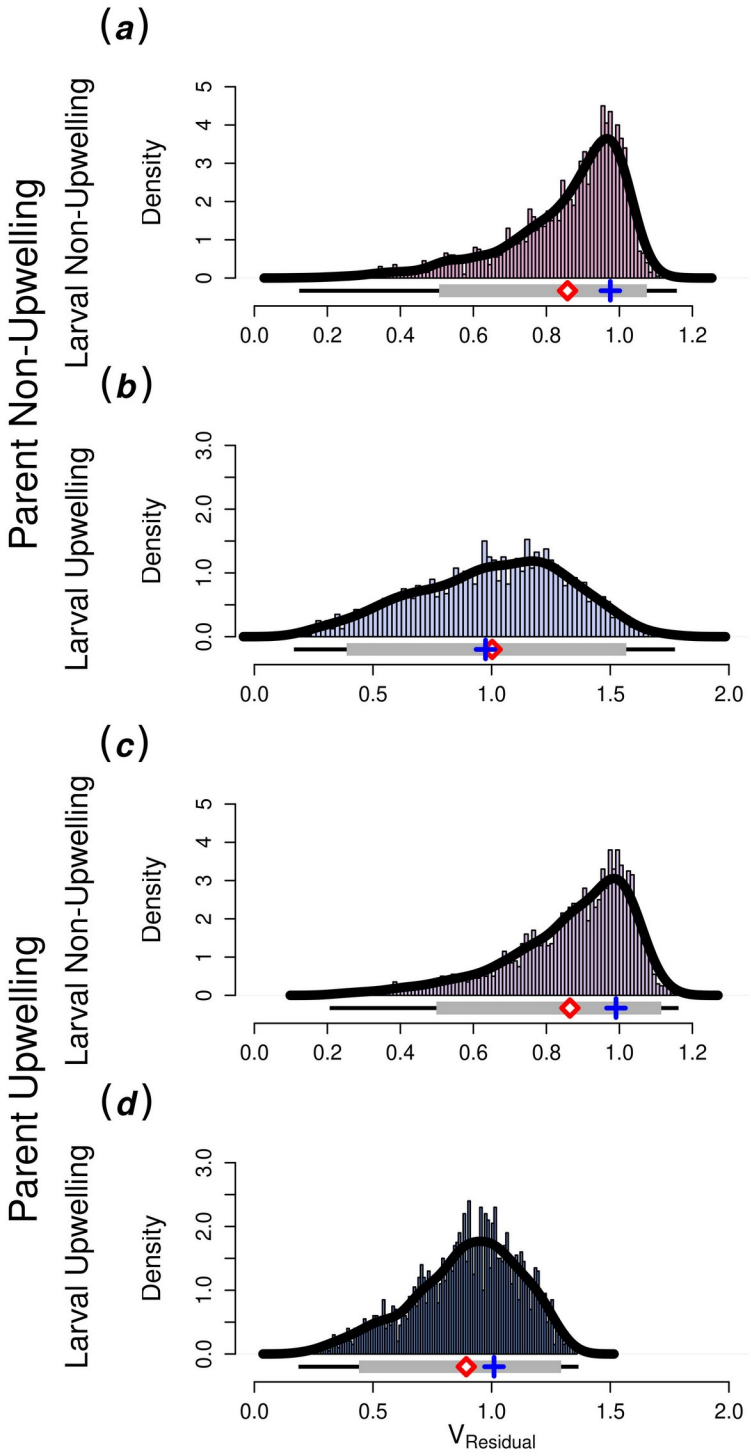

Figure S5. *S. purpuratus* spicule length marginal posterior distributions of residual variances. Plotting lines and symbols are described in the legend to Figure S3.

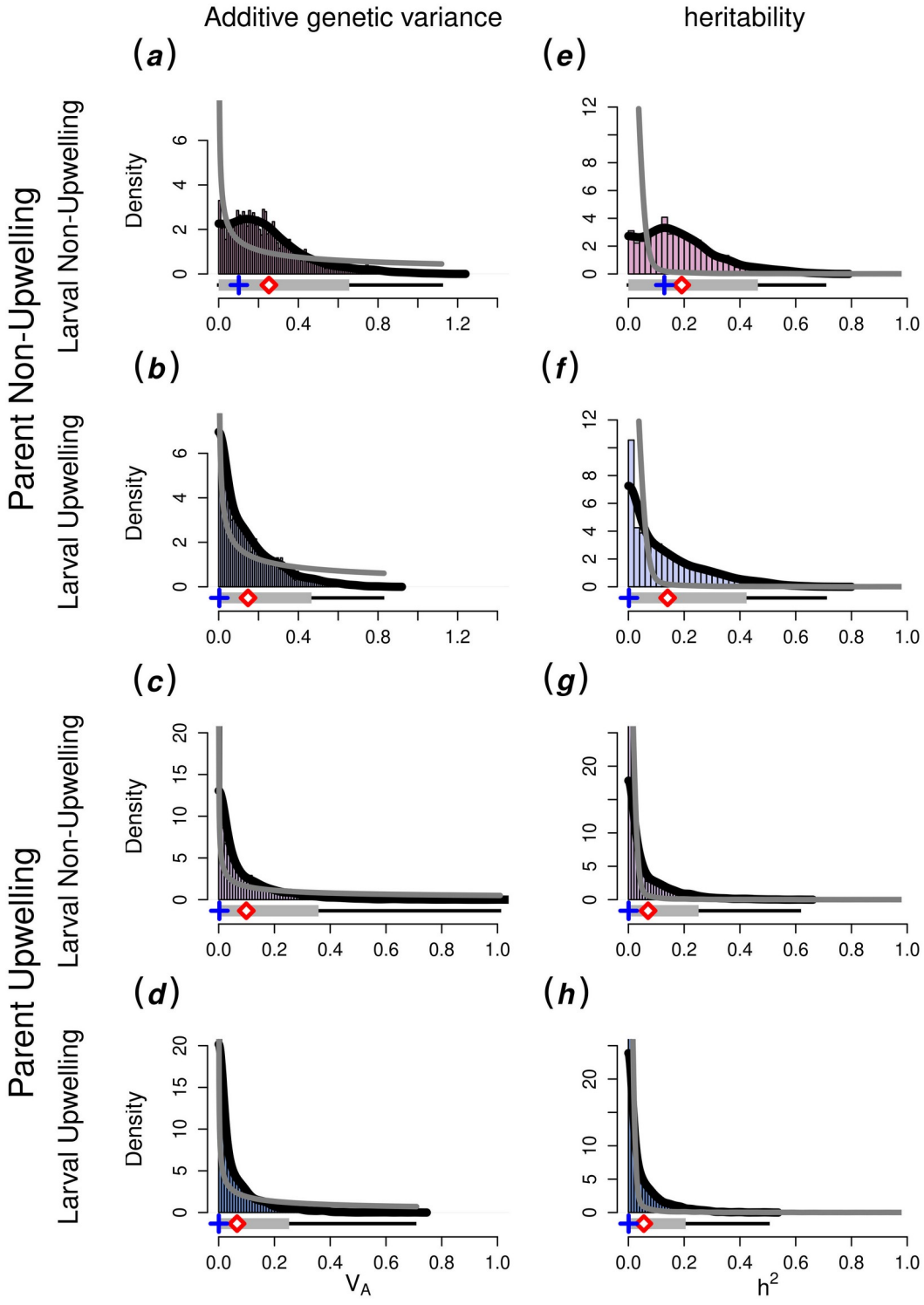

Figure S6: *S. purpuratus* body length marginal posterior MCMC samples, kernel density estimate, and prior density for the additive genetic variance (V_A) (*a-d*) and heritability (h^2) (*e-h*). Plotting lines and symbols are described in the legend to Figure S3.

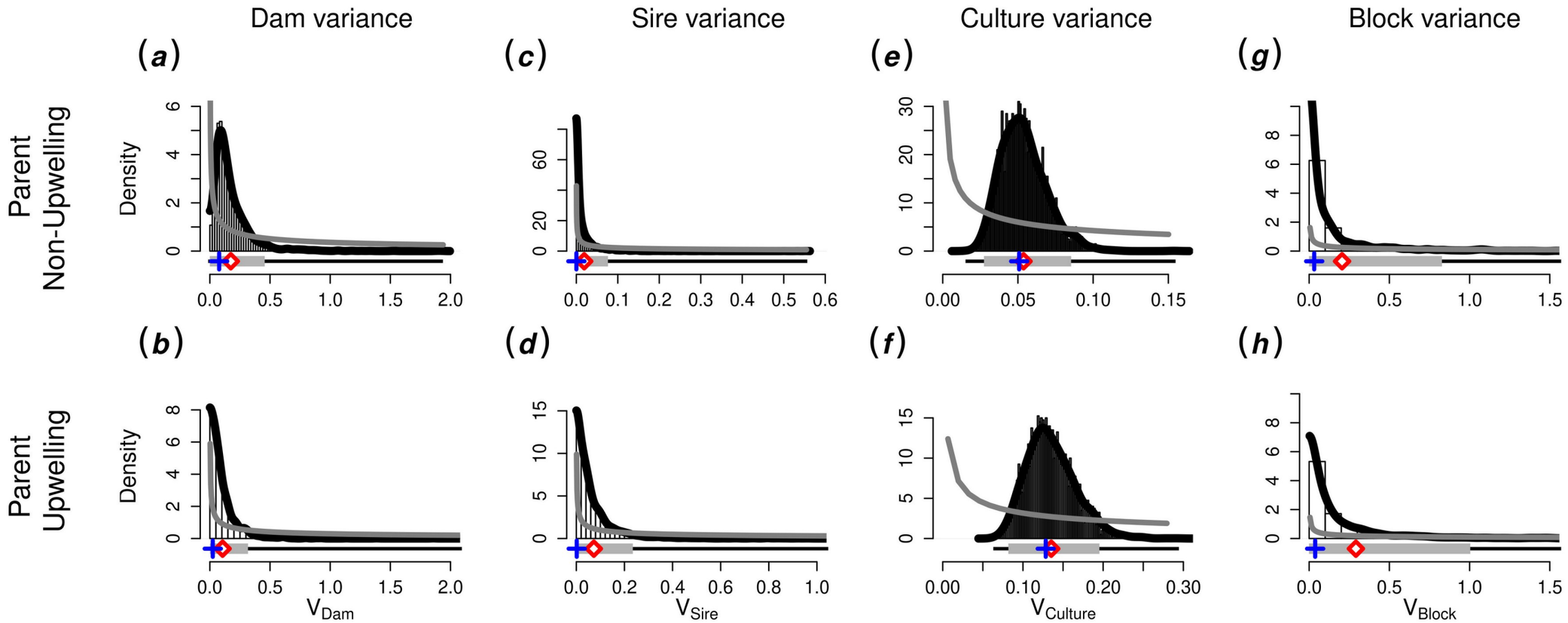

Figure S7. *S. purpuratus* body length marginal posterior MCMC samples (histogram bars), density (black line), and prior density (grey line) for the dam (*a*-*b*), sire (*c*-*d*), culture (*e*-*f*), and block (*g*-*h*) variances. Plotting lines and symbols are described in the legend to Figure S3.

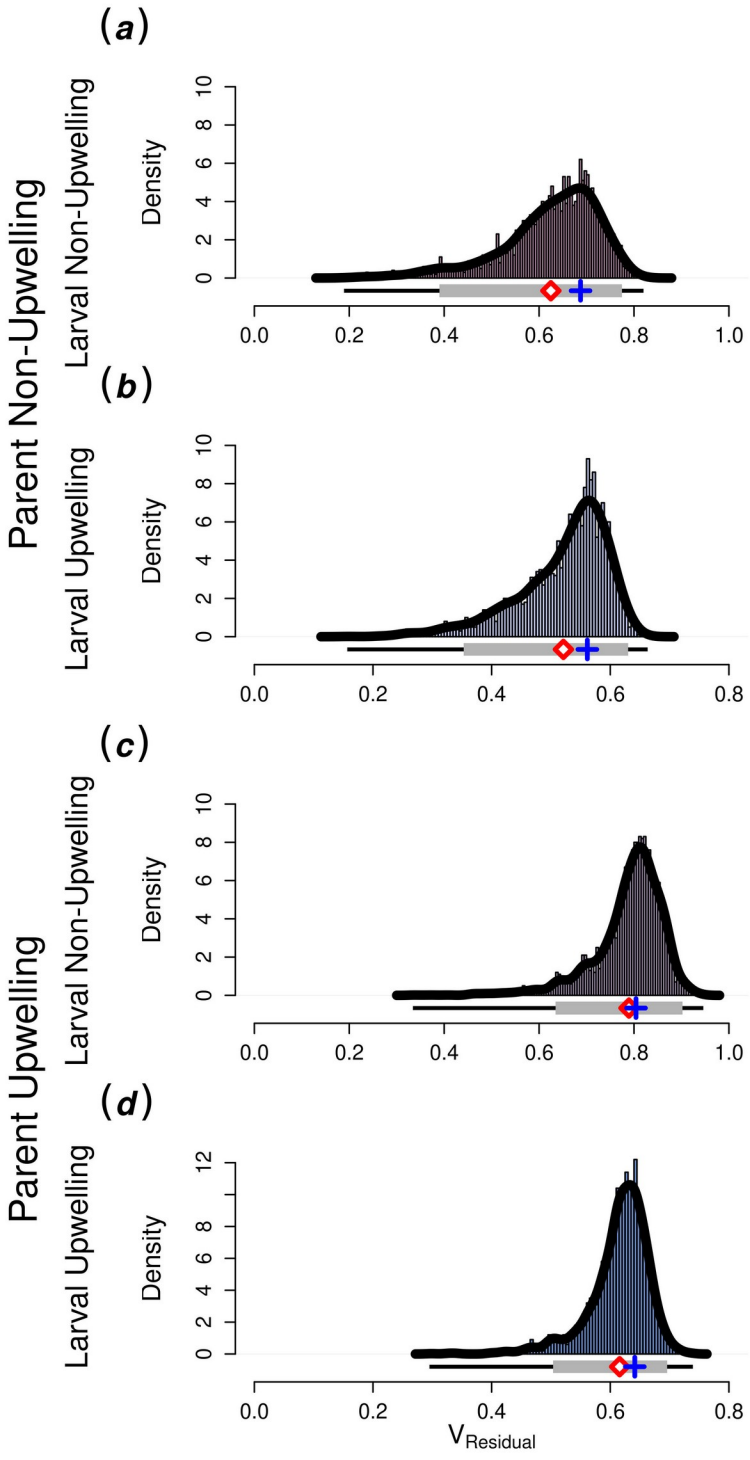

Figure S8. *S. purpuratus* body length marginal posterior distributions of residual variances. Plotting lines and symbols are described in the legend to Figure S3.

6. Family mean additive genetic value posterior distributions

To interpret our estimates of cross-environment additive genetic correlations, we ranked family mean additive genetic values for comparison between larval rearing environments. To calculate these ranks, we calculated marginal posterior distributions of family mean additive genetic values (i.e., using the model predicted random effects associated with the additive genetic (co)variance terms) for larvae in each rearing environment. We then chose the posterior mode as the best representation of the family mean additive genetic value and ranked these values among the 20 families in each larval rearing environment and parental conditioning environment combination.

The posterior mode was the best value to represent the marginal posterior distribution of family mean additive genetic value, because these posterior distributions were generally leptokurtic and often skewed (Figures S9-S16). Thus, the modal value represented a parameter value with much higher posterior probability than other values in the distribution, especially compared to the posterior mean when these distributions were skewed.

Figures S9 to S16 below.

Spicule Length

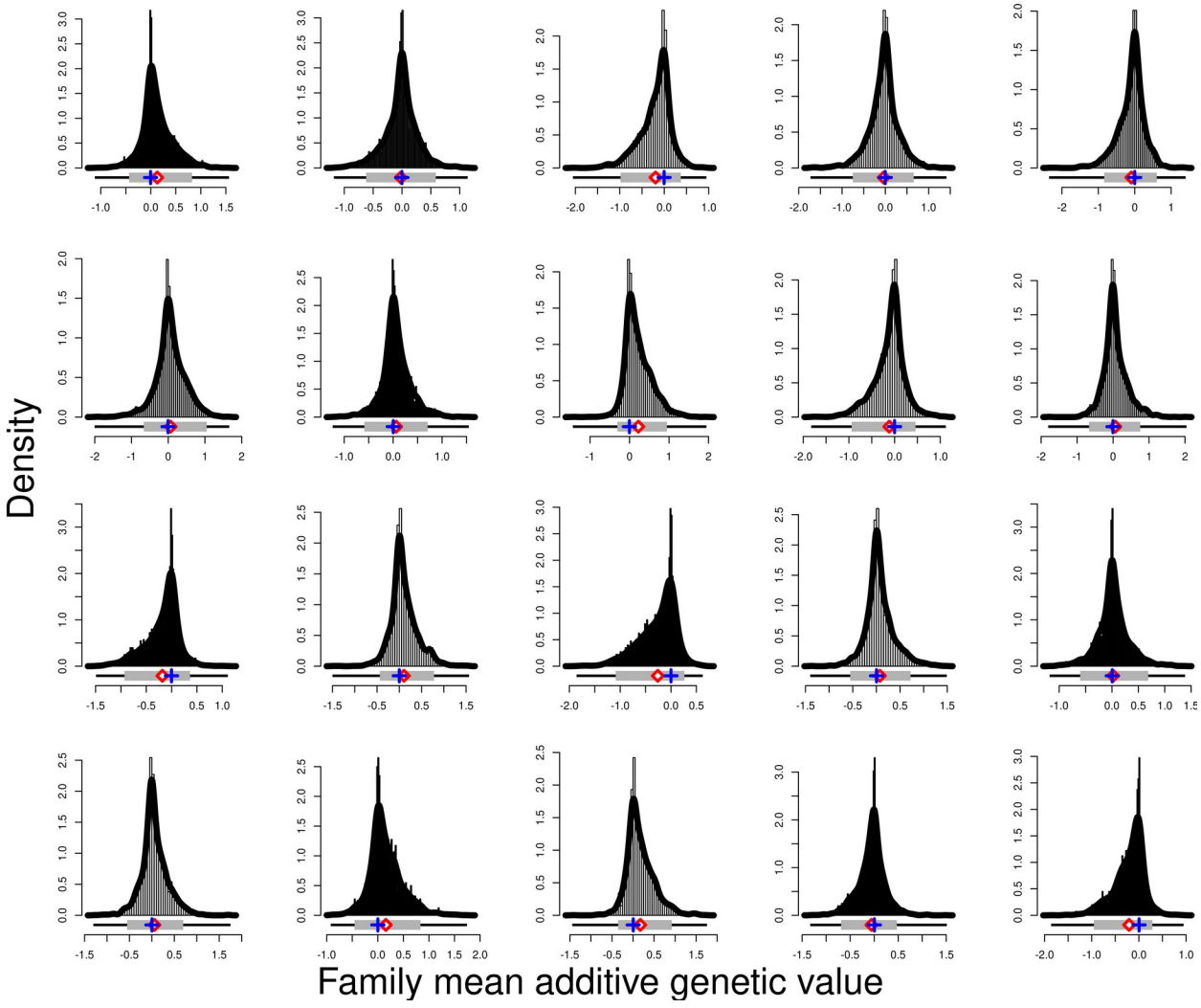

Figure S9. *S.purpuratus* spicule length family mean additive genetic value marginal posterior distributions for each family where parents were conditioned in the Non-Upwelling environment and larvae developed in the Non-Upwelling environment. Plotting lines and symbols are described in the legend to Figure S3.

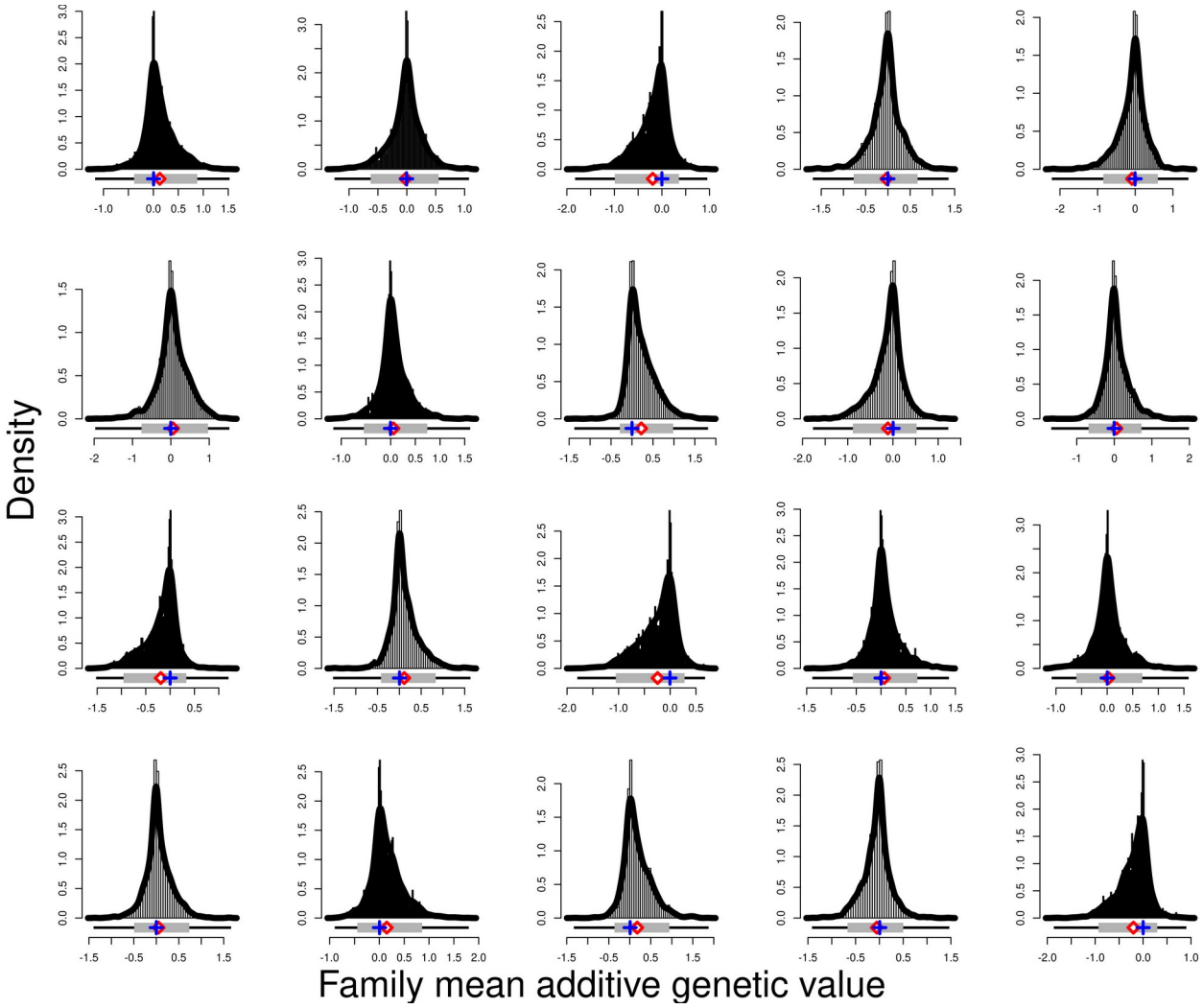

Figure S10. *S.purpuratus* spicule length family mean additive genetic value marginal posterior distributions for each family where parents were conditioned in the Non-Upwelling environment and larvae developed in the Upwelling environment. Plotting lines and symbols are described in the legend to Figure S3.

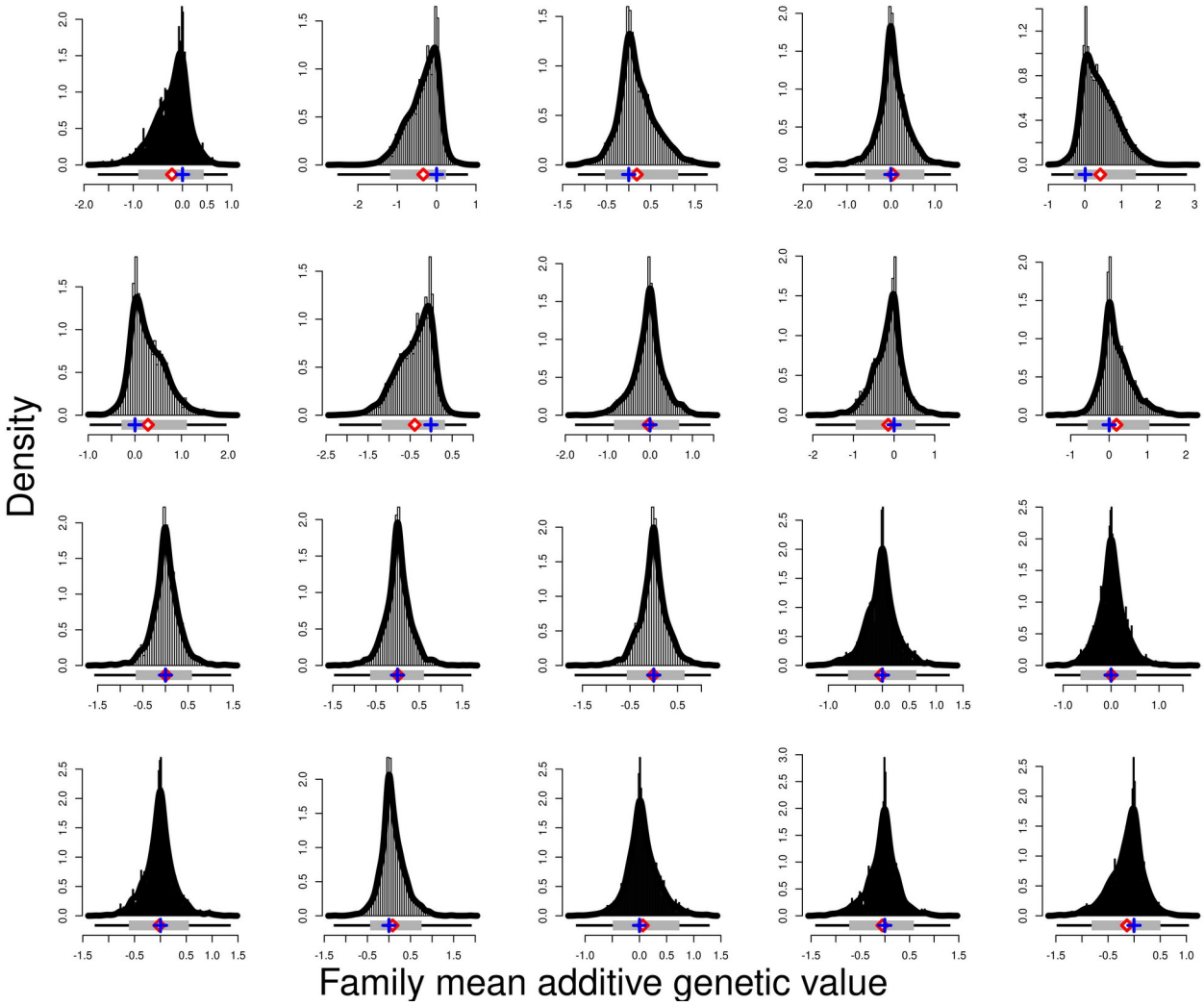

Figure S11. *S.purpuratus* spicule length family mean additive genetic value marginal posterior distributions for each family where parents were conditioned in the Upwelling environment and larvae developed in the Non-Upwelling environment. Plotting lines and symbols are described in the legend to Figure S3.

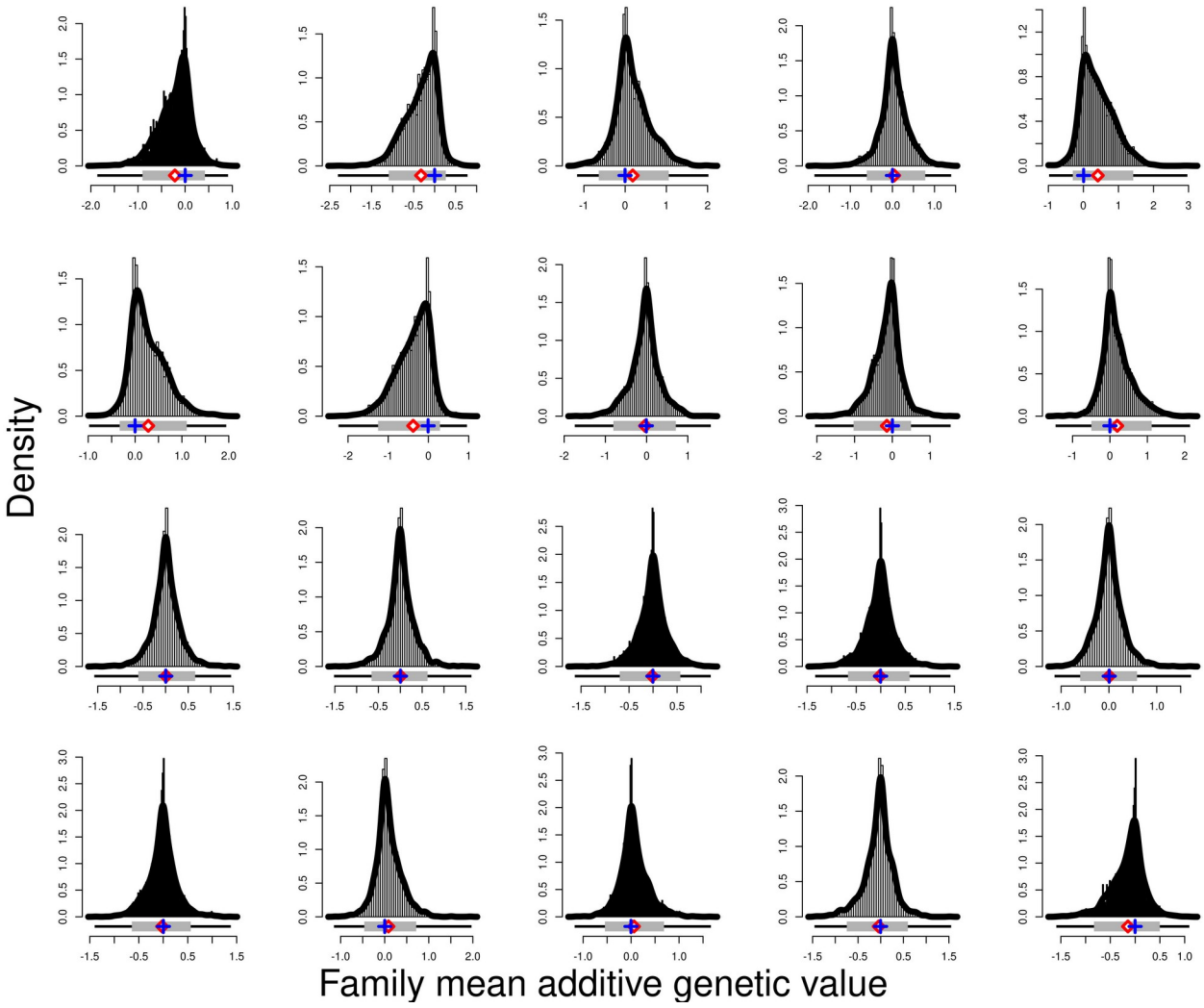

Figure S12. *S.purpuratus* spicule length family mean additive genetic value marginal posterior distributions for each family where parents were conditioned in the Upwelling environment and larvae developed in the Upwelling environment. Plotting lines and symbols are described in the legend to Figure S3.

Body Length

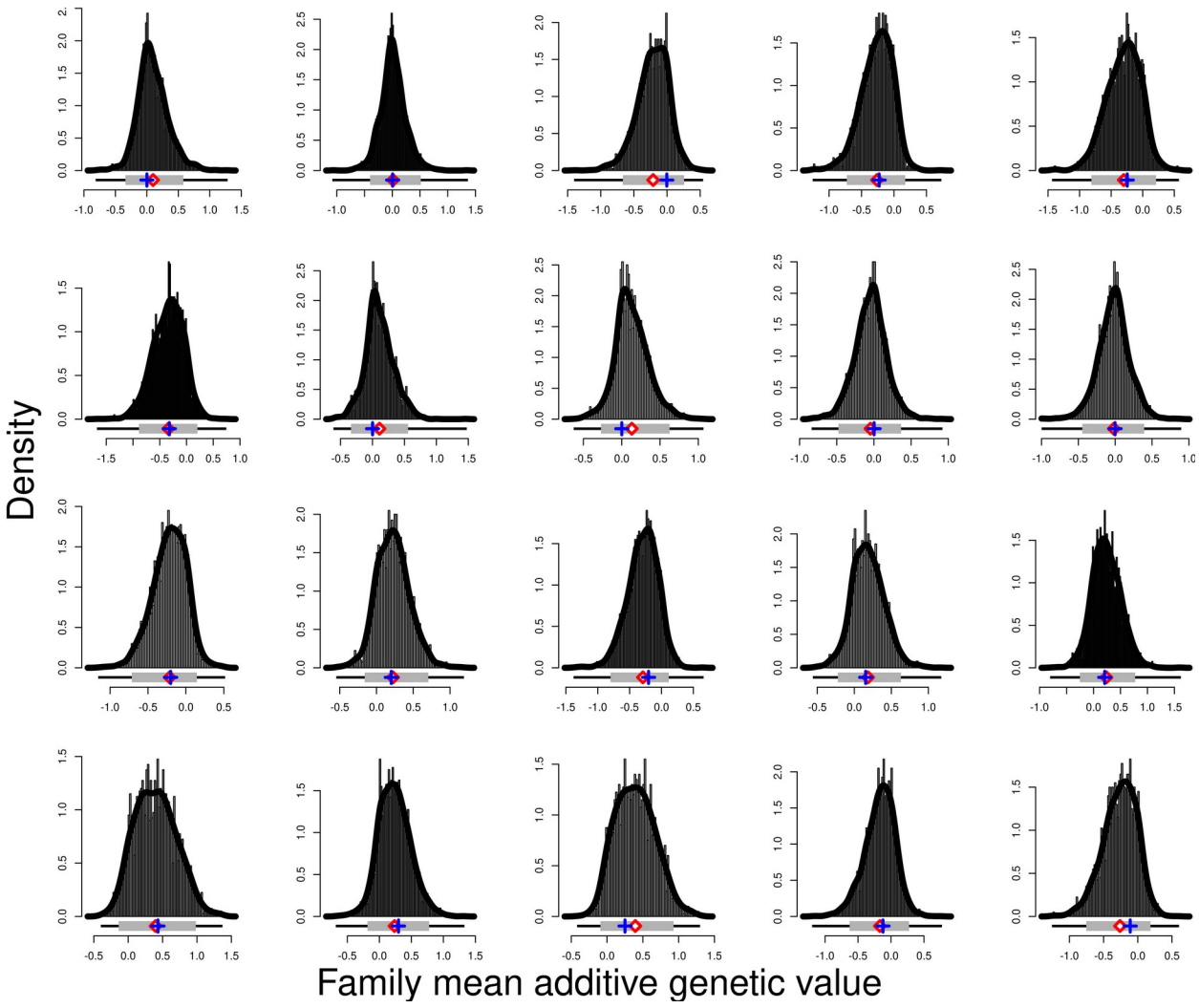

Figure S13. *S.purpuratus* body length family mean additive genetic value marginal posterior distributions for each family where parents were conditioned in the Non-Upwelling environment and larvae developed in the Non-Upwelling environment. Plotting lines and symbols are described in the legend to Figure S3.

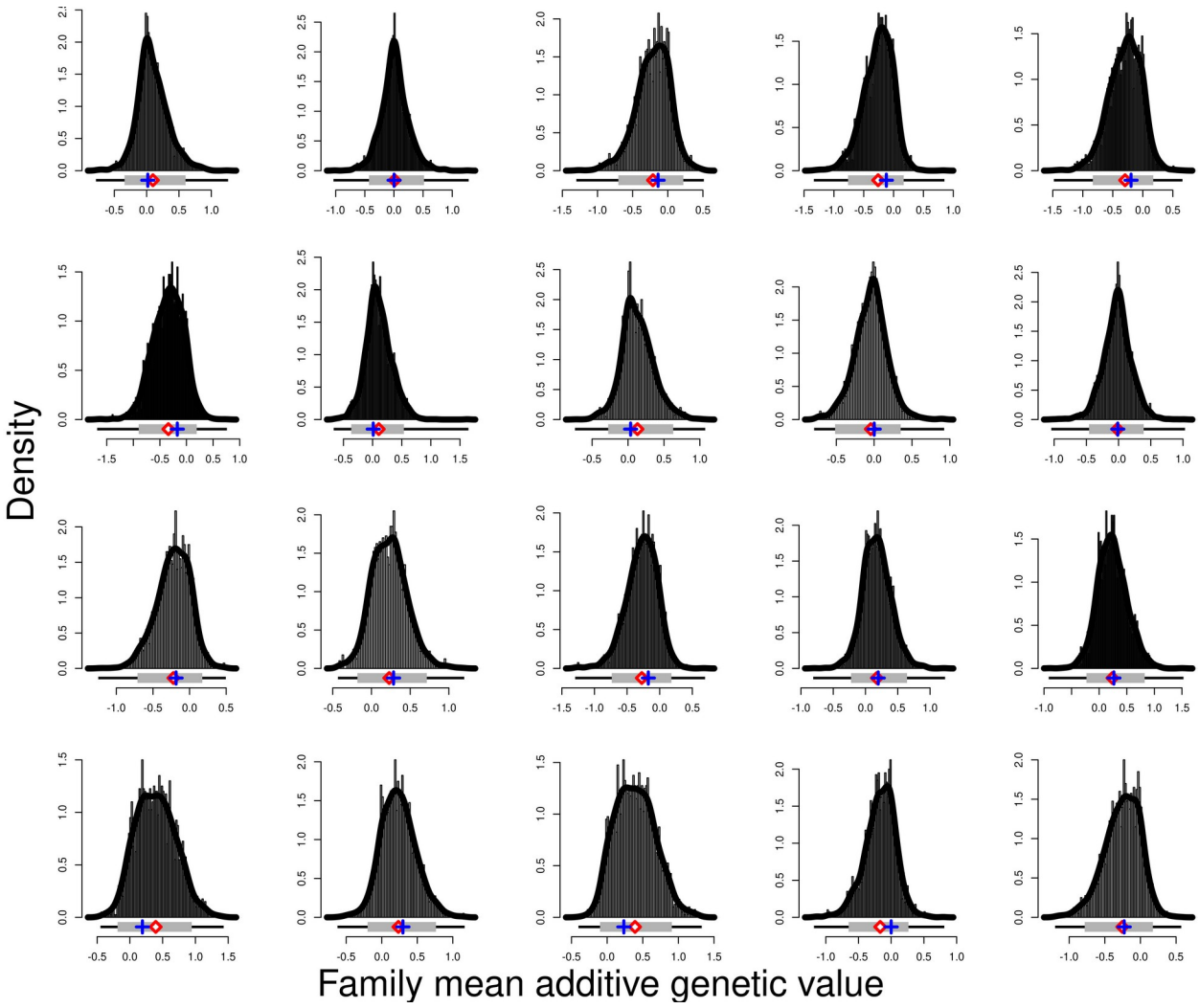

Figure S14. *S.purpuratus* body length family mean additive genetic value marginal posterior distributions for each family where parents were conditioned in the Non-Upwelling environment and larvae developed in the Upwelling environment. Plotting lines and symbols are described in the legend to Figure S3.

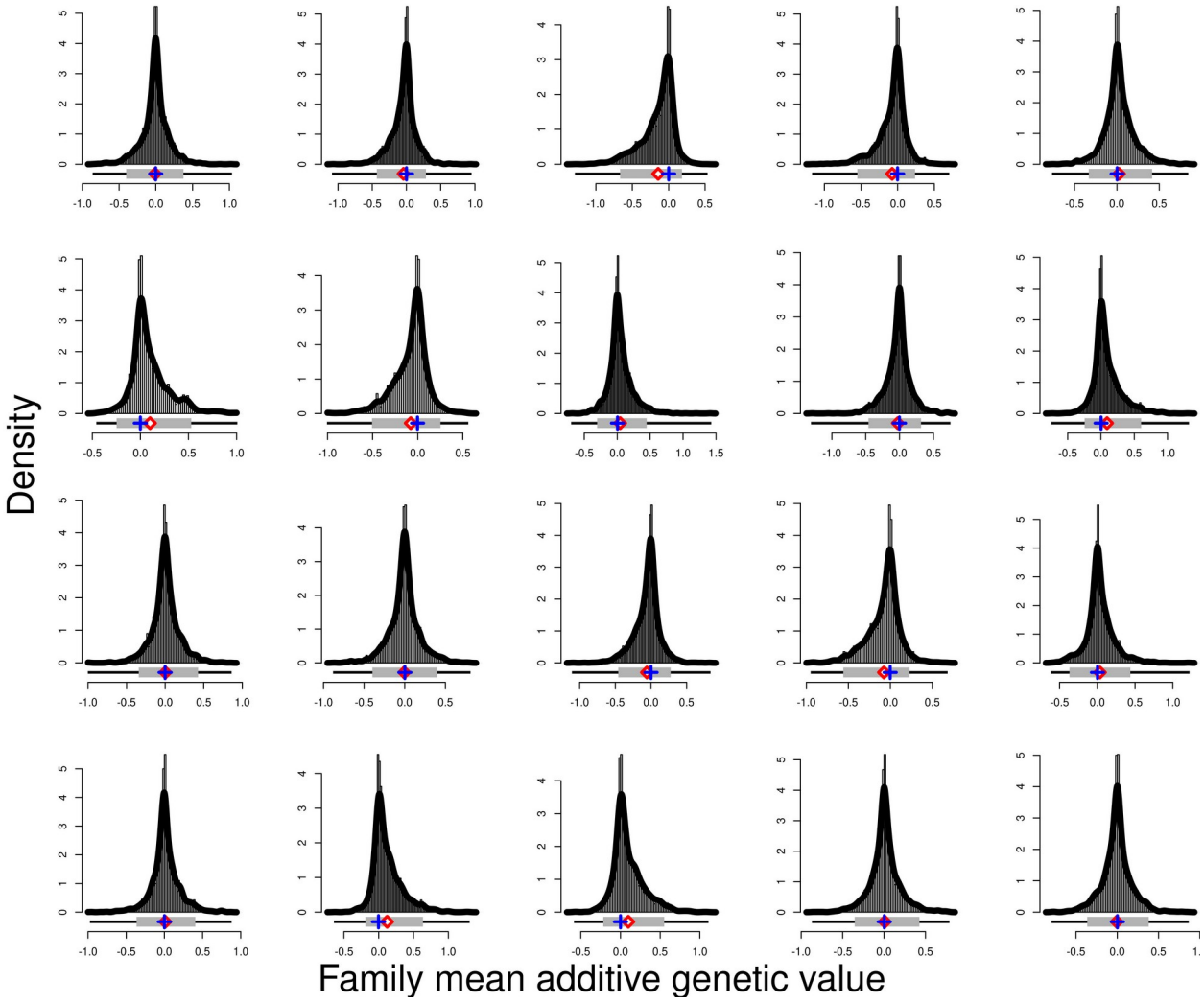

Figure S15. *S.purpuratus* body length family mean additive genetic value marginal posterior distributions for each family where parents were conditioned in the Upwelling environment and larvae developed in the Non-Upwelling environment. Plotting lines and symbols are described in the legend to Figure S3.

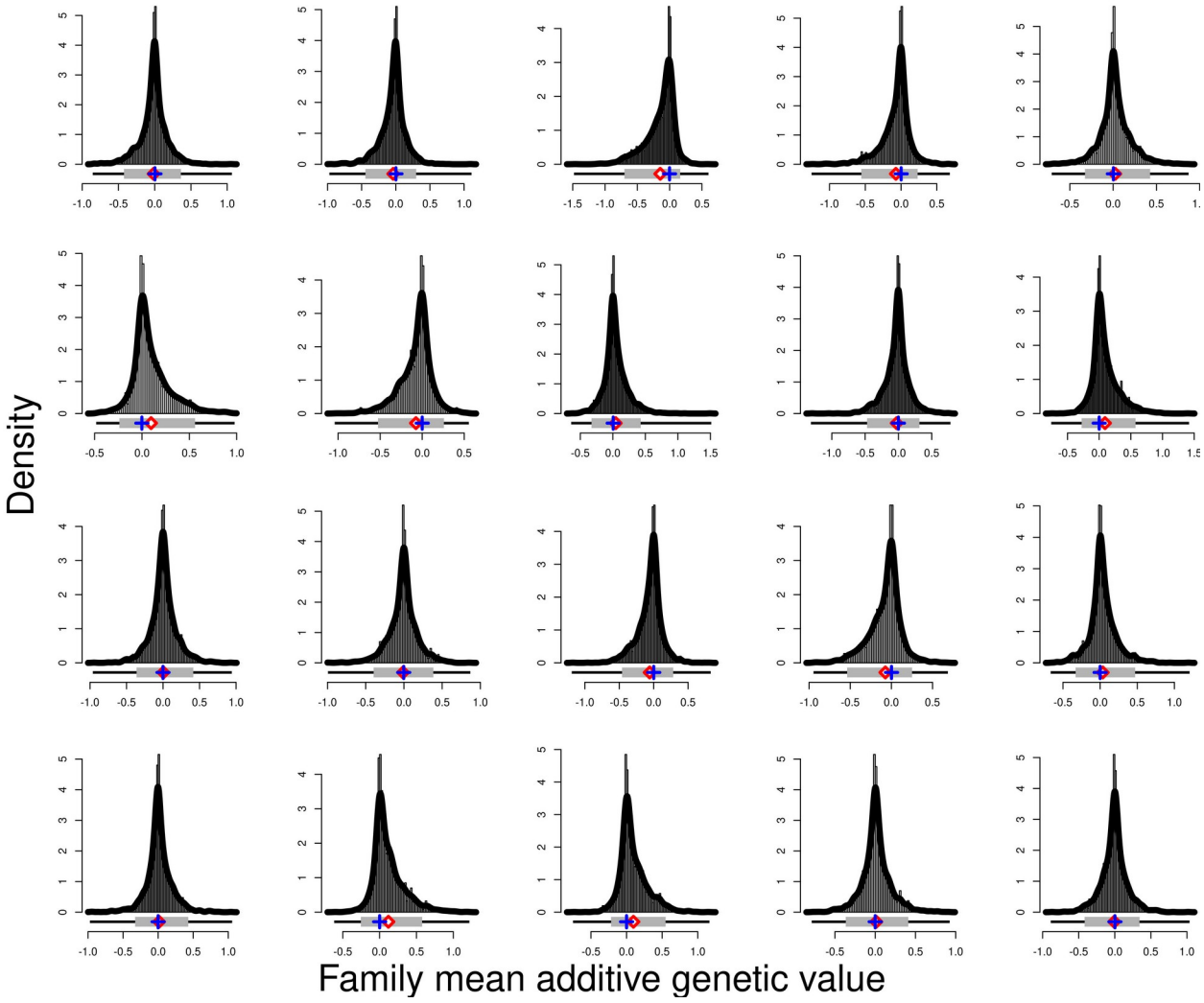

Figure S16. *S.purpuratus* body length family mean additive genetic value marginal posterior distributions for each family where parents were conditioned in the Upwelling environment and larvae developed in the Upwelling environment. Plotting lines and symbols are described in the legend to Figure S3.